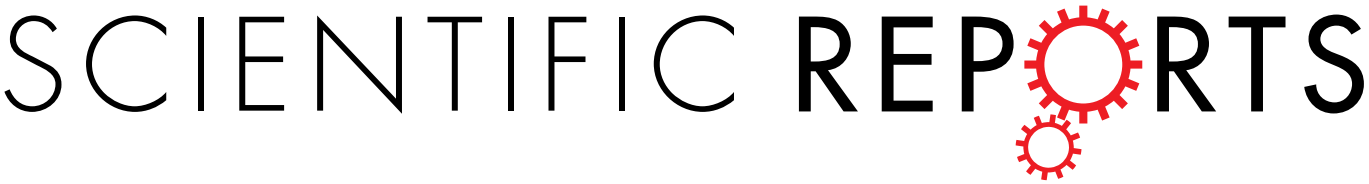

OPEN

Analysis and modeling of Fano resonances using equivalent circuit elements

Received: 06 June 2016
Accepted: 28 July 2016
Published: 22 August 2016

Bo Lv[1], Rujiang Li[2], Jiahui Fu[1], Qun Wu[1], Kuang Zhang[1], Wan Chen[1], Zhefei Wang[1] & Ruyu Ma[1]

Fano resonance presents an asymmetric line shape formed by an interference of a continuum coupled with a discrete autoionized state. In this paper, we show several simple circuits for Fano resonances from the stable-input impedance mechanism, where the elements consisting of inductors and capacitors are formulated for various resonant modes, and the resistor represents the damping of the oscillators. By tuning the pole-zero of the input impedance, a simple circuit with only three passive components e.g. two inductors and one capacitor, can exhibit asymmetric resonance with arbitrary *Q*-factors flexiblely. Meanwhile, four passive components can exhibit various resonances including the Lorentz-like and reversely electromagnetically induced transparency (EIT) formations. Our work not only provides an intuitive understanding of Fano resonances, but also pave the way to realize Fano resonaces using simple circuit elements.

Fano resonance has received much attention due to the interesting physics such as distinctly asymmetric shape and high quality-factor (*Q*-factor)[1]. The interference of a discrete autoionized state with a continuum gives rise to characteristically asymmetric peaks in excitation spectra, which can be extended to the resonance scattering of quantum theory[2–4]. Recently, the classical oscillator systems enabled by plasmonic nanostructures and metamaterials have led to the achievement of asymmetric Fano-type transmission/reflection in the optical frequencies, which has open up a new perspective towards achieving high-precision nanoscale sensors[5–9]. Furthermore, the steep *Q*-factor profile promises applications in bio/chemical sensors[10–13].

A discrete autoionized state and a continuum can be analogue of a broadband-bright mode and a narrowband-dark mode depending on the coupled approach with the incident light from free space[14]. The bright mode has a large scattering cross section and a low quality factor due to the radiation coupling, which is always excited directly by external energy. On the contrary, the dark mode normally has a significantly larger quality factor, which is only limited by the loss performance and excited indirectly by the bright mode[15]. The formation exhibits the interference phenomena, where constructive interference corresponds to resonant enhancement and destructive interference to resonant suppression of the transmission[16,17]. Furthermore, The circuit system which is an effective-mapping image of the classical mechanics can be devoted to the mechanism of Fano resonance[18]. In passive electric system, the inductance represents a behavior increasing with higher frequency in spectra domain, and the capacitance effects the opposite process. Accordingly, the electric resonance is the equilibrium state when the functionality of inductance and capacitance are balance. Based on this, the electric-dynamic equations of the 'bright' and 'dark' electric-resonant modes are established and imitate Fano resonance effectively. Nevertheless, the circuit structures of high-*Q*-factor resonances consist of numerous orders of electric resonances, and the solutions of dynamic-differential equations are extremely complicated. Therefore, the ultimate goal of simple structure and an effectively steady-convenient analysis of Fano-like resonance are highly desired.

In this paper, we formulate the series and parallel circuits consisting of inductors and capacitors for various-resonant modes, and the resistor represents the damping of the oscillators. Additionally, we propose the stable-input impedance mechanism of passive circuit system to mimic the functionality of the Fano resonance. Based on this theory, the pole-zero adjustment of the input impedance can implement arbitrary *Q*-factor asymmetric resonance flexiblely in simple circuit system which consists of only three passive components (such as two inductors and one capacitor). Furthermore, various resonances (such as Lorentz-like and reversely EIT

[1]Microwave and Electromagnetic Laboratory, Harbin Institute of Technology, No.92, Xidazhi Street, Nangang District, Harbin City, Heilongjiang Province, China. [2]College of Information Science and Electronic Engineering, Zhejiang University, Hangzhou 310027, China. Correspondence and requests for materials should be addressed to B.L. (email: lb19840313@126.com) or R.L. (email: rujiangli@zju.edu.cn) or J.F. (email: fjh@hit.edu.cn)

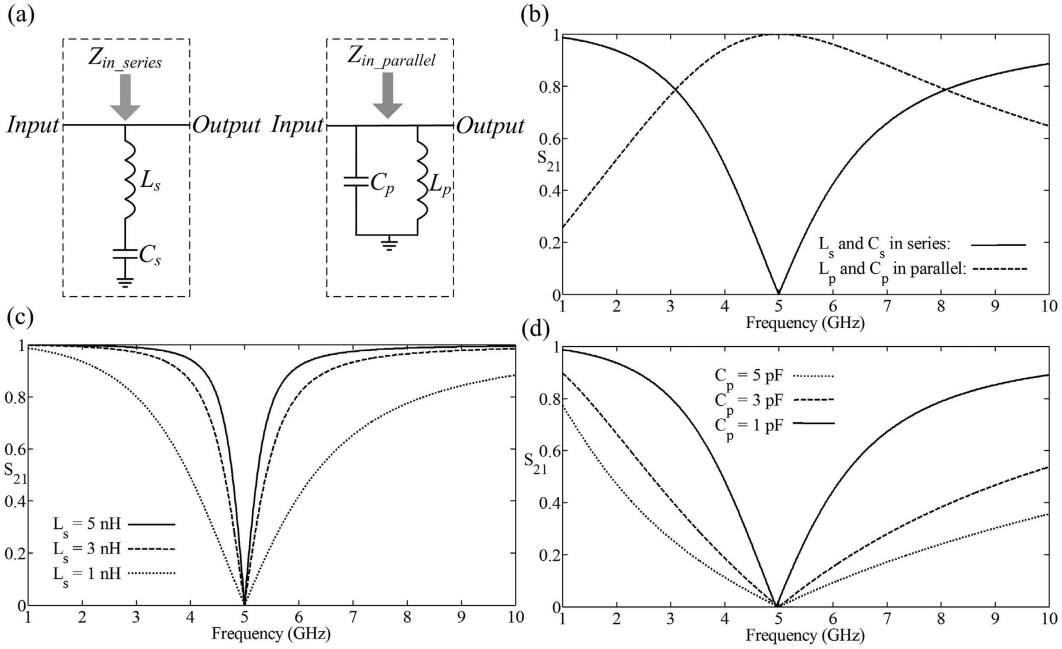

Figure 1. (**a**) The schematic of the series and parallel-*LC* circuit as the branch parallel in the main-energy thread. Here the inductors are $L_s = L_p = 1.0132\,nH$, and the capacitors are $C_s = C_p = 1\,pF$. (**b**) The transmittance S_{21} of the series and parallel-*LC* circuit system, for the series-circuit branch parallel in system, the reflected-resonant frequency $\omega = 1/\sqrt{L_s C_s} = 5GHz$, and the parallel-circuit branch parallel in system, the transparent-resonant frequency $\omega = 1/\sqrt{L_p C_p} = 5GHz$. (**c**) The transmittance of series circuit with various $L_s = 5\,nH$, $3\,nH$, $1\,nH$ and the corresponding capacitor $C_s = 0.2026\,pF$, $0.3377\,pF$, $1.1032\,pF$ containing the resonant frequency $\omega_{s0} = 5\,GHz$. (**d**) The transmittance of parallel circuit with various $C_p = 5\,pF$, $3\,pF$, $1\,pF$ and the corresponding inductor $L_p = 0.2026\,nH$, $0.3377\,nH$, $1.1032\,nH$ containing the resonant frequency $\omega_{p0} = 5\,GHz$.

formations) can be imitated by four electric components. This approach has well-defined Fano-like effective properties and opens up the possibilities to construct extremely high-*Q*-factor devices while maintaining the simplification of the system. Besides, they can be a guidance for design in microwave or optical circuits and, in particular, for periodic artificial electromagnetic materials. Additionally, it is interesting to note that the passive circuit approach and the theoretical propositions presented in this work processes to achieve high-precision and compressed-composition components[19].

Fano resonances without damping

First, we consider Fano resonances without damping, where the circuits are schematically shown in Fig. 1(a). We calculate the stable-input impedance of the circuit which is embedded in the single-input-single-output (SISO) system[20], and tune its pole-zero[21]. The transmittance is defined as $S_{21} = P_{output}/P_{input}$, where P_{input} and P_{output} are the incident and transmitted power, respectively. The stable-input impedance of series inductor-capacitor (*LC*) circuit and parallel *LC* circuit are given as

$$Z_{in\_series}(\omega) = \frac{jL_s(\omega - \omega_{s0})(\omega + \omega_{s0})}{\omega}, \tag{1}$$

and

$$Z_{in\_parallel}(\omega) = -\frac{j\omega}{C_p(\omega - \omega_{p0})(\omega + \omega_{p0})}, \tag{2}$$

respectively, where the resonant frequencies $\omega_{s0/p0} = 1/\sqrt{L_{s/p}C_{s/p}} = 5\text{GHz}$ depend on the inductor $L_{s/p} = 1.0132\,nH$ and the capactor $C_{s/p} = 1\,pF$. In Eq. (1), the stable-input impedance of series *LC* circuit Z_{in_series} has the zeros $\omega = \pm\omega_{s0}$ and the poles $\omega = 0$. Here, the negative frequency $\omega = -\omega_{s0}$ are ignored due to its physical-meaningless. Then, the input impedance of series circuit is shorted to the ground at the zero $\omega = \omega_{s0}$, which leads the input energy total reflected and the transmittance is lowest $S_{21} = 0$ as the solid line in Fig. 1(b). In Eq. (2), the input-impedance function of parallel *LC* circuit has the zero $\omega = 0$, and the poles $\omega = \pm\omega_{p0}$. Excluding the physical-meaningless pole $\omega = -\omega_{p0}$, the input-impedance of parallel *LC* circuit is infinite at the pole point $\omega = \omega_{p0}$ and the transmittance is all-pass $S_{21} = 1$ as the dashed line in Fig. 1(b). From Eq. (1, 2), the steep in the vicinity of ω_{s0} and ω_{p0} is proportional to the inductor L_s in the series circuit, and inversely proportional to the capacitor C_p in the LC-parallel circuit. Therefore, the Q factor can be adjusted by the inductor L_s and the capacitor

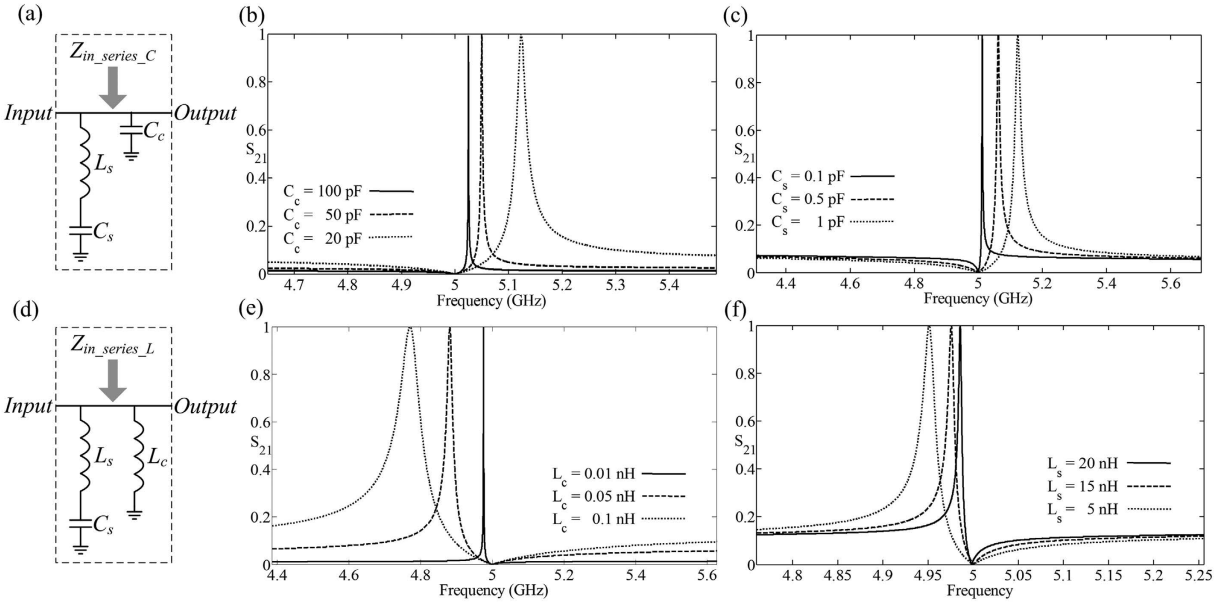

Figure 2. (**a**) The schematic of the complementary capacitor C_c parallel in the series LC circuit. (**b**) The transmittance of the circuit system in Fig. 2(a) with different complementary capacitor $C_c = 20\,pF$, $50\,pF$ and $100\,pF$. (**c**) The transmittance of the circuit system in Fig. 2(a) with different series capacitor $C_s = 0.1\,pF$, $0.5\,pF$ and $1\,pF$. (**d**) The schematic of the complementary inductor L_c parallel in the series LC circuit. (**e**) The transmittance of the circuit system in Fig. 2(d) with different complementary inductor $L_c = 0.1\,nH$, $0.05\,nH$ and $0.01\,nH$. (**f**) The transmittance of the circuit system in Fig. 2(d) with different series inductor $L_s = 5\,nH$, $15\,nH$ and $20\,nH$.

C_p as shown in Fig. 1(c,d), meanwhile, the corresponding capacitor C_s and inductor L_p is modified for the remaining of resonant frequency $\omega_{0s/p} = 5$ GHz.

Here the Q-factor is expressed as $Q = \omega_0/(\omega_H - \omega_L)$, where ω_0 is the central resonant frequency, and ω_L, ω_H are the half-amplitude frequencies lower and higher than ω_0. In Fig. 1(c), the series-LC Q-factor are 10.8, 6.5 and 2 for the various inductor $L_s = 5\,nH$, $3\,nH$ and $1\,nH$. which presents the series-LC resonance sharper with decreasing series inductor L_s. In Fig. 1(d), the parallel-LC Q-factor are 2.27, 1.36 and 0.45 for the various capacitor $C_p = 5\,pF$, $3\,pF$ and $1\,pF$, which presents the parallel-LC resonance sharper with increasing parallel capacitor C_p.

Based on the above analysis, we can build the Fano-like asymmetric resonance by a series-LC circuit which represents the narrowband-dark mode coupling with a capacitor or an inductor as the broadband-bright mode, as shown in Fig. 2(a,d). Here we use the stable-input impedance method instead of oscillators-dynamic equations in spectra domain to reveal the mechanism of the asymmetric-coupling modes. In Fig. 2(a), the complementary capacitor C_c is added parallel to the series-LC resonance, and the the stable-input impedance of this circuit system is:

$$Z_{in\_series\_C} = -\frac{j}{\omega C_c}\frac{(\omega - \omega_{s0})(\omega + \omega_{s0})}{(\omega - \omega_{s0}\sqrt{(C_s/C_c) + 1})(\omega + \omega_{s0}\sqrt{(C_s/C_c) + 1})} \tag{3}$$

Abandoning the physical meaningless solutions, we get the pole of stable-input impedance $\omega_{s0}\sqrt{(C_s/C_c) + 1}$ in Eq. (3) which is greater than the zero ω_{s0}. In addition, the zeros and poles are corresponding to the reflect and transparent resonant frequencies respectively in main-energy thread. Therefore, the transmittance can steep down to zero ω_{s0} at the higher-frequent pole $\omega_{s0}\sqrt{(C_s/C_c) + 1}$ with the coefficient $\sqrt{(C_s/C_c) + 1} \to 1$, and presents the formation of Fano-like asymmetric resonance and and high-Q factor. Further, we can get the infinite-Q-factor by turning the pole greatly close to the zero through increasing the complementary capacitor C_c and decreasing the series capacitor C_s. Here we maintain the series-resonant frequency $\omega_{s0} = 5\,GHz$, and increase the complementary capacitor $C_c = 20\,pF$, $50\,pF$, $100\,pF$, that leads to the transparent resonance $5.132\,GHz$, $5.050\,GHz$ and $5.025\,GHz$ closing to the reflect resonance $\omega_{s0} = 5\,GHz$ gradually, and the resonance becomes sharper, as shown in Fig. 2(b). When the complementary capacitor $C_c = 20\,pF$ and decreasing the series capacitor $C_s = 1\,pF$, $0.5\,pF$, $0.1\,pF$, under the conditions of the series inductor L_s changing correspondingly for maintaining the series-resonant frequency $\omega_{s0} = 5\,GHz$, the transparent resonance is $5.132\,GHz$, $5.062\,GHz$, $5.013\,GHz$ closing to the reflect resonance $\omega_{s0} = 5\,GHz$ gradually, and the Q-factor becomes higher, as shown in Fig. 2(c).

The complementary inductor L_c is parallel-added in the series-LC circuit, as shown in Fig. 2(d), and the the stable-input impedance is:

$$Z_{in\_series\_L} = \frac{j\omega L_s L_c}{(L_s + L_c)}\frac{(\omega - \omega_{s0})(\omega + \omega_{s0})}{(\omega - \omega_{s0}/\sqrt{((L_c/L_s) + 1)})(\omega + \omega_{s0}/\sqrt{((L_c/L_s) + 1)})} \tag{4}$$

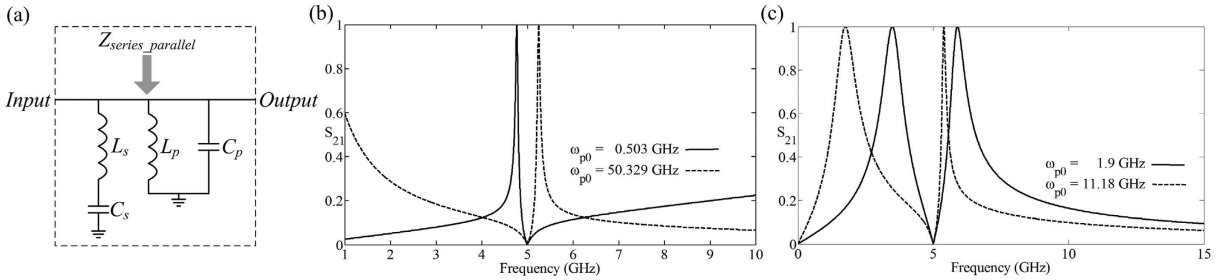

Figure 3. (**a**) The schematic of the series and parallel resonant circuits are parallel in the main-energy thread. (**b**) The transmittance of the circuit system in Fig. 3(a) with different parallel-resonant frequencies $\omega_{p0} = 0.503\,GHz$, $50.329\,GHz$. (**c**) The transmittance of the circuit system in Fig. 3(a) with different parallel-resonant frequencies $\omega_{p0} = 1.9\,GHz$, $11.18\,GHz$.

Abandoning the physical meaningless solutions, we get the pole $\omega_{s0}/\sqrt{(L_c/L_s)+1}$ in Eq. (4) lower than the zero ω_{s0}. Therefore, the transmittance can steep down to zero at the pole $\omega_{s0}/\sqrt{(L_c/L_s)+1}$ located lower than the zero ω_{s0} when the coefficient $\sqrt{(L_c/L_s)+1} \to 1$, and presents the formation of Fano-like asymmetric resonance. Further, we can get the infinite-Q-factor by turning the pole point close to the zero point through decreasing the complementary inductor L_c and decreasing the series inductor L_s. Here we maintain the series-resonant frequency $\omega_{s0} = 5\,GHz$, and decrease the complementary inductor $L_c = 0.1\,nH$, $0.05\,nH$, $0.01\,nH$, that leads the transparent resonance $4.770\,GHz$, $4.881\,GHz$, $4.976\,GHz$ closes to the reflect resonance $\omega_{s0} = 5\,GHz$ gradually, and the Q-factor becomes higher, as shown in Fig. 2(e). When the complementary capacitor $L_c = 0.1\,nH$ is constant and increasing the series inductor $L_s = 5\,nH$, $15\,nH$, $20\,nH$, under the conditions of the series inductor changing correspondingly for maintaining the series-resonant frequency $\omega_{s0} = 5\,GHz$, the transparent resonance is $4.951\,GHz$, $4.976\,GHz$, $4.986\,GHz$ closing to the reflect resonance $\omega_{s0} = 5\,GHz$ gradually, and the Q-factor becomes higher, as shown in Fig. 2(f).

In Fig. 2(b), the Q-factor is 2513, 1263 and 197 for $C_c = 100\,pF$, $50\,pF$ and $20\,pF$, which presents the resonance sharper with the increasing the complementary capactor C_c. In Fig. 2(c), the Q-factor is 1671, 361.6 and 197.1 for $C_s = 0.1\,pF$, $0.5\,pF$ and $1\,pF$, which presents the resonance sharper with decreasing the series capacitor C_s. In Fig. 2(e), the Q-factor is 4976, 203.4 and 51.85 for $L_c = 0.01\,nH$, $0.05\,nH$ and $0.1\,nH$, which presents the resonance sharper with decreasing the complementary inductor L_c. In Fig. 2(f), the Q-factor is 831, 712 and 225 for $L_s = 20\,nH$, $15\,nH$ and $5\,nH$, which presents the resonance sharper with increasing the complementary inductor L_s.

We build the series and parallel resonant circuits parallel in the main-energy thread as shown in Fig. 3(a), and analyze the stable-input impedance:

$$Z_{series\_parallel} = \frac{j\omega}{C_p} \frac{(\omega - \omega_{s0})(\omega_1 + \omega_{s0})}{(\omega - \omega_A)(\omega - \omega_B)(\omega + \omega_A)(\omega + \omega_B)} \tag{5}$$

where the poles expressed as $\omega_A = \sqrt{\left(\omega_{s0}^2 + 2\omega_{p0}^2 + \sqrt{\omega_{s0}^4 + 4\omega_{p0}^4}\right)/2}$ and $\omega_B = \sqrt{\left(\omega_{s0}^2 + 2\omega_{p0}^2 - \sqrt{\omega_{s0}^4 + 4\omega_{p0}^4}\right)/2}$. Here we maintain the series-circuit elements $L_s = 1.0132\,nH$, $C_s = 1\,pF$ and thus the series-resonant frequency $\omega_{s0} = 5\,GHz$. Abandoning the physical meaningless solutions, when the series and parallel resonant frequencies satisfying $\omega_{p0} \ll \omega_{s0}$, the pole ω_B of Eq. (5) satisfies $\omega_B \approx 0$, and the other pole ω_A is little higher than the zero ω_{s0}. Therefore, the closing of pole and zero can construct transparent-asymmetric and high-Q-factor resonance. Based on the above analysis, we can set the parallel elements $L_p = 1.1032\,nH$, $C_p = 0.1\,pF$and thus the parallel-resonant frequency $\omega_{p0} = 0.503\,GHz$. which leads to the transparent resonant frequency $\omega_B = 5.246\,GHz$ closing to the zero ω_{s0}, shown as the dashed line in Fig. 3(b). When the series and parallel resonant frequencies satisfying $\omega_{p0} \gg \omega_{s0}$, the pole $\omega_A \approx \sqrt{2}\,\omega_{p0}$ is far from ω_{s0}, and the other pole $\omega_B \approx \omega_{s0}$ is little lower than the zero ω_{s0} in Eq. (5) which constructs the transparent-asymmetric and high-Q-factor resonance. We set the parallel elements $L_p = 0.1\,nH$, $C_p = 0.1\,pF$ and thus the parallel-resonant frequency $\omega_{p0} = 50.329\,GHz$, which leads to the transparent resonant frequency $\omega_B = 4.768\,GHz$ closing to the zero ω_{s0}, shown as the solid line in Fig. 3(b). When we set the parallel elements $L_p = 1.0132\,nH$, $C_p = 7\,pF$, and parallel-resonant frequency $\omega_{p0} = 1.9\,GHz$. Thus, from the solution of Eq. (5), the pole $\omega_B = 4.753\,GHz$ is located lower than the zero ω_{s0} which forms the Lorentz-like resonance, and the other pole $\omega_A = 6.392\,GHz$ is little higher than the zero ω_{s0} which forms the transparent-asymmetric and high-Q-factor resonance, shown as the dashed line in Fig. 3(c). When the poles $\omega_{s0} - \omega_B = \omega_A - \omega_{s0}$ distribute even around the zero ω_{s0}, the two resonant frequencies locate asymmetric and a sharp reflect-resonance is formed at the zero ω_{s0} which is likely a converse reversely EIT formation. Here we set the parallel elements $L_p = 0.2993\,nH$and $C_p = 5\,pF$, thus, the the parallel resonant frequency $\omega_{p0} = 4.1144\,GHz$. The transparent resonant frequencies $\omega_A = 5.895\,GHz$, $\omega_B = 3.49\,GHz$, which forms two mirror symmetrical resonance, as shown the solid line in Fig. 3(c), and the reflect resonance $\omega_{s0} = 5\,GHz$ is also like a reversely EIT phenomenon.

The asymmetric resonance with damping

Here we add the resistors R_s, R_c as damping in the series resonant circuit consisting of the series inductor $L_s = 1.0132\,nH$, the series capacitor $C_s = 1\,pF$ and the complementary capacitor $C_s = 20\,pF$, as shown in Fig. 4(a).

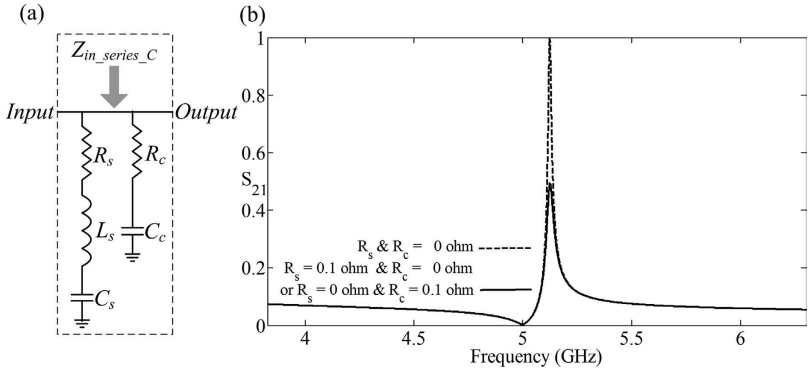

Figure 4. The schematic of the complementary capacitor $C_c = 20\,pF$ parallel in the series LC circuit consisting of the series inductor $L_s = 1.0132\,nH$ and the series capacitor $C_s = 1\,pF$ with damping which is represented by the resistors R_s and R_c. (**b**) The transmittance of the circuit system in Fig. 4(a) with different resistors $R_s = 0.1\,ohm$ and $R_c = 0.1\,ohm$.

We set the resistor $R_s = 0.1\,ohm$ and $R_c = 0.1\,ohm$ respectively, which leads to the amplitude of the transmittance is lower than no-damping, but the shape of the asymmetric resonance remains unchanged, as shown in Fig. 4(b).

Conclusion

In conclusion, we show that the Fano resonance can be interpreted as an analogy with the stable-input impedance mechanism by taking passive circuit system as an example. Based on the circuit theory, only three passive components (such as two inductors and one capacitor) can mimic arbitrary *Q*-factor asymmetric resonance flexiblely by adjusting the pole-zero of the impedance. Furthermore, four passive components can imitate the various resonance (such as Lorentz-like and reversely EIT formations). Besides, our work provides an intuitive understanding of the Fano resonance using briefly electric formation and processes to achieve high-precision by compressed-composition components.

References

1. Miroshnichenko, A. E. *et al.* Fano resonance: A discovery that was not made 100 years ago. *Opt. Phot. News* **19,** 48 (2008).
2. Fano, U. Effects of configuration interaction on intensities and phase shifts. *Phys. Rev.* **124,** 1866–1878 (1961).
3. Johnson, A. C., Marcus, C. M., Hanson, M. P. & Gossard, A. C. Coulombmodified Fano resonance in a one-lead quantum dot. *Phys. Rev. Lett.* **93,** 106803 (2004).
4. Kobayashi, K., Aikawa, H., Sano, A., Katsumoto, S. & Iye, Y. Fano resonance in a quantum wire with a side-coupled quantum dot. *Phys. Rev. B* **70,** 035319 (2004).
5. Fan, S. H. Sharp asymmetric line shapes in side-coupled waveguide-cavity systems. *Appl. Phys. Lett.* **80,** 908–910 (2002).
6. Genet, C., van Exter, M. P. & Woerdman, J. P. Fano-type interpretation of red shifts and red tails in hole array transmission spectra. *Opt. Commun.* **255,** 331–336 (2003).
7. Hao, F. *et al.* Symmetry breaking in plasmonic nanocavities: Subradiant LSPR sensing and a tunable Fano resonance. *Nano Lett.* **8,** 3983–3988 (2008).
8. Rybin, M. V. *et al.* Fano resonance between Mie and Bragg scattering in photonic crystals. *Phys. Rev. Lett.* **103,** 023901 (2009).
9. A. Attaran *et al.* Circuit Model of Fano Resonance on Tetramers, Pentamers, and and Broken Symmetry Pentamers. *Plasmonics.* **9,** 1–11 (2014).
10. Yang. Y., I. I. Kravchenko, D. P. Briggs & J. Valentine. All-dielectric metasurface analogue of electromagnetically induced transparency. *Nat Commun.* **5,** 5753 (2014).
11. N. Liu *et al.* Planar metamaterial analogue of electromagnetically induced transparency for plasmonic sensing. *Nano Lett.* **10,** 1103–1107 (2010).
12. C. Debus & P. H. Bolivar. Terahertz biosensors based on double split ring arrays. P*roc. SPIE.* 6987, 6987OU (2008).
13. B. Lahiri, A. Z. Khokhar, D. L. Rue, R. M. McMeekin & S. G, N. P. Johnson. Asymmetric split ring resonantors for optical sensing of organic materials. *Opt. Express.* **17,** 1107–1115 (2009).
14. Luk'yanchuk, B. *et al.* The Fano resonance in plasmonic nanostructures and metamaterials. *Nat. Mater.* **9,** 707–715 (2010).
15. Y. S. Joe *et al.* Classical analogy of Fano resonances. *Phys. Scr.* **74,** 259–266 (2006).
16. A. E. Miroshnichenko, S. Flach & Y. S. Kivshar. Fano resonances in nanoscale structures. *Rev Mod Phys.* **82,** 2577 (2010).
17. M. I. Tribelsky & A. E. Miroshnichenko. Giant in-particle field concentration and Fano resonances at light scattering by high-refractive-index particles. *Phys. Rev. A.* **93,** 053837 (2016).
18. Fan, S. H., Suh, W. & Joannopoulos, J. D. Temporal coupled-mode theory for the Fano resonance in optical resonators. *J. Opt. Soc. Am. A* **20,** 569–572 (2003).
19. Ruan, Z. & Fan, S. Temporal coupled-mode theory for Fano resonance in light scattering by a single obstacle. *J. Phys. Chem. C* **114,** 7324–7329 (2009).
20. N. Ayllón, A. Anakabe, J. M. Collantes., G. Soubercazc-Pun & S. Forestier. Sensitivity Enhancement in Pole-Zero Identification Based Stability Analysis of Microwave Circuits. *Integr. Nonlinear Microw. Millim-Wave Circuits Workshop*, Malaga, Spain, Nov. 75–78 (2008).
21. A. Anakabe, N. Ayllón, J. M. Collantes, A. Mallet, G. Soubercaze-Pun & K. Narendra. Automatic Pole-Zero Identification for Multivariable Large-Signal Stability *Analysis of RF and Microwave Circuits*. (2010)

Author Contributions

B.L. proposed the main method and theory of the manuscript. B.L. and R.L. wrote the main manuscript text. J.F., Q.W. and K.Z. reviewed the manuscript. W.C., Z.W. and R.M. prepared Figures 1–4.

Additional Information

Competing financial interests: The authors declare no competing financial interests.

How to cite this article: Lv, B. *et al.* Analysis and modeling of Fano resonances using equivalent circuit elements. *Sci. Rep.* **6**, 31884; doi: 10.1038/srep31884 (2016).